Cathodoluminescence of Zinc Sulfide Films Grown by Single Source Chemical Vapor Deposition

E. Y. M. Lee, N. H. Tran, J. J. Russell,* and R. N. Lamb

Surface Science and Technology Centre, University of New South Wales, Sydney, Australia

Received: November 25, 2003; In Final Form: March 12, 2004

The cathodoluminescent properties of zinc sulfide films prepared via single-source chemical vapor deposition of zinc dimethyldithiocarbamate under a variety of precursor fluxes were examined. X-ray photoelectron spectroscopy and depth profiling of the resultant films found bulk carbon impurities of <1% atomic concentrations. X-ray diffraction indicated that the films have a single (111) orientation. Cathodoluminescence spectroscopy found that the light-emitting properties of the films were strongly dependent on the film deposition conditions, with certain films producing a strong band gap emission on a broad background spectrum, while others produced only defect emissions. Transmission electron microscopy indicated that structural defects in the form of threading defects were responsible for the loss of edge emission while carbon contamination at the grain boundaries led to a broad emission in the visible region. Overall the results suggest that ZnS thin films grown using a low cost and straightforward technique such as single-source chemical vapor deposition may have potential applications in producing light-emitting devices.

I. Introduction

One of the advantages of zinc sulfide as a semiconductor material is its strongly luminescent properties.[1−4] However, producing zinc sulfide thin films through standard techniques such as sputter deposition, evaporative deposition, and solution deposition can be difficult due to the problems associated with sulfur sources. This is because elemental sulfur is a solid at room temperature and the most common gaseous source of sulfur, hydrogen sulfide, is a toxic gas.

Due to these film deposition problems, the potential ZnS thin film applications have not been fully realized. Recently, single-source chemical vapor deposition (SSCVD) has been used to grow highly crystalline cubic ZnS films.[5−12] In SSCVD the zinc and sulfur sources are located within the precursor with additional organic ligands attached to increase volatility. Deposition is achieved by subliming the precursor in a vacuum onto a hot substrate where it decomposes with the loss of the organic groups to form zinc sulfide.

Crystallographic structure and morphology are critically important in the luminescent process. A thin film will typically have different cathodoluminescent properties compared to a single crystal since the former will have defects. Defects can affect the cathodoluminescence (CL) in one of two ways: either by quenching the luminescence or emitting at a different wavelength. It is possible for a defect to do both by absorbing light at one wavelength and emitting at a higher one. Although inter-granular zones may play a role in the structurally-based properties of thin films, the focus in this study is on crystallographic defects and not the role of inter-granular zones. This is because in the context of this study the role of inter-granular zones may be less critical for a number of reasons: 1) the ZnS films in this study are highly crystalline and the grains/crystallites are quite large;[12] 2) the penetration depth of the electron beam in CL is greater than the thickness of the films, and 3) ZnS has a relatively high UV−vis transparency. As a result of these three factors, the majority of light emission that will be observed will originate from the bulk of the film (from within the crystallites) and not just the surface or the inter-granular zones.

The aim of this study is to examine the light-emitting properties of ZnS thin films produced by single source CVD, to determine the underlying reasons for the light emission in terms of structure, and to evaluate the potential of these films in device applications.

II. Experimental Section

ZnS films were produced by depositing zinc dimethyldithiocarbamate (Aldrich) in a high vacuum chamber with a background pressure of 2×10^{-7} torr. The precursor partial pressure used in this study varied from $\sim 2 \times 10^{-5}$ to $\sim 2 \times 10^{-4}$ torr. The substrate (silicon 100 wafers) was maintained at a fixed temperature of 425 °C. Film growth times were roughly 2−8 h with a corresponding thickness of 0.5−2 μm. X-ray diffraction (XRD) was carried out using a PW 3040/60 X'Pert Pro Diffractometer with a Cu Kα source ($\lambda = 1.5418$ Å). Scanning electron microscopy (SEM) was performed using a Hitachi 4500 Microscope. Transmission electron microscopy (TEM) was performed on a Philips CM200 field emission gun transmission electron microscope. Cross-sectional sample thinning for TEM analysis was prepared with a FEI xP200 focused ion beam mill. Cathodoluminescence measurements were performed using an Oxford Instruments MonoCL system attached to a JEOL 35C SEM with a 30 keV beam energy. An fcc (110) oriented ZnS single crystal was used as a reference for CL analysis.

Monte Carlo simulations were performed with the Casino v2.42 program (obtained from Université de Sherbrooke, Québec, Canada). Calculations were performed based on a 2000 electron trajectory with a beam energy of 30 keV.

* To whom correspondence should be addressed. E-mail: jen.russell@unsw.edu.au.

10.1021/jp037583u CCC: $27.50
Published on Web 05/25/2004

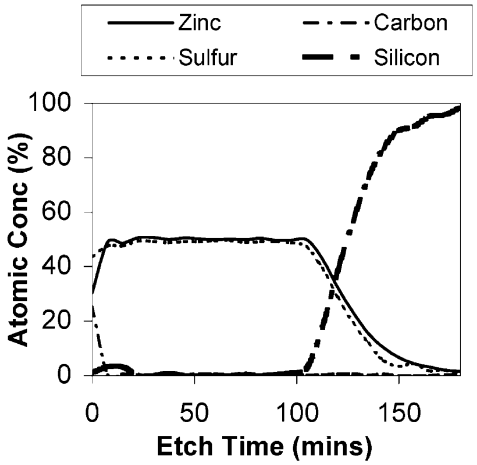

Figure 1. Atomic concentrations of Zn, S, C, and Si in an XPS depth profile of a ZnS film grown on a silicon wafer.

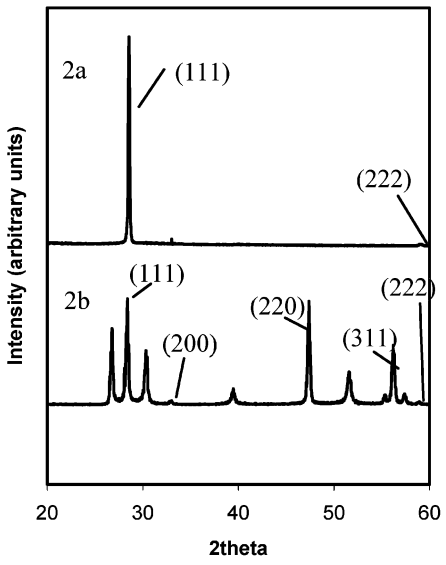

Figure 2. X-ray Diffraction patterns of: 2a) (111) oriented ZnS film and 2b) a ZnS powder sample containing both hexagonal and cubic phases.

III. Results and Discussion

The chemical composition of the films was determined through XPS depth profiling. Figure 1 is a typical depth profile of a ZnS film grown through single-source CVD. The carbon concentration at the film surface (~26%) was predominantly adventitious hydrocarbons from the precursor and exposure to atmosphere postdeposition. Almost all of this carbon was removed after the Ar+ etching procedure with the subsequent carbonaceous impurity remaining below 1% atomic concentration throughout the bulk of the film. The Zn:S atomic ratios also remained stoichiometric within the bulk of the film. Varying the precursor flux within the range of this experiment did not have any significant effect on the chemical composition of the films with the bulk carbon content of all films in this study < 1%.

The XRD of a typical film is labeled in Figure 2a, along with an XRD of a ZnS powder containing both hexagonal and cubic crystallites (Figure 2b). Note that only the reflections for the cubic phase of ZnS are labeled since it has been established in previous studies that ZnS films grown through this method of single-source CVD have a cubic structure.[12] Compared to Figure 2b, the XRD in Figure 2a contains a single reflection indicating that the film has a single fcc (111) orientation. XRD performed on all the films in this study found no other orientations present, with near-identical wide scan diffractograms.

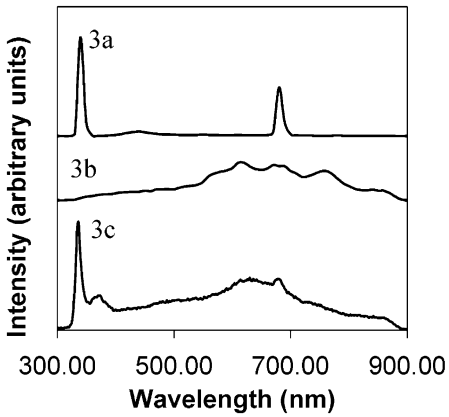

Figure 3. Cathodoluminescence spectra of: 3a) ZnS single crystal, 3b) a ZnS film with no band-gap emission, and 3c) a ZnS film with a strong band-gap emission.

When CL measurements were performed, all the films showed CL emission although the shape of the spectra varied greatly. Figure 3a shows the CL spectrum of a zinc sulfide single crystal. The features present are the band edge emission at ~340 nm (~ 3.64 eV), the secondary harmonic (~680 nm) which is an artifact of the Bragg grating and a small amount of defect structure seen in the broad peak from 400 to 500 nm. In contrast Figure 3b is the CL spectrum of a film grown for 2 h at maximum precursor flux (10^{-4} torr). In this spectrum there is no distinct band gap emission, only a broad and continuous background. In contrast, Figure 3c is the CL spectrum of the ZnS film grown at minimum flux (2×10^{-5} torr) for 8 h. The resultant spectrum of this film contains a strong band gap emission at ~336 nm (~ 3.69 eV) observed in the single crystal, a secondary peak at ~368 nm (~ 3.37 eV) and a broad peak at ~636 nm (~ 1.95 eV) as well as the continuous background emission observed in Figure 3b. The band gap values observed in both the single-crystal reference and the film in Figure 3c are in good agreement with the literature value for ZnS of 3.68 eV.[13] Furthermore, there is no significant peak broadening of the band gap emission for the film in Figure 3c compared to the single crystal, confirming the high-quality nature of the film. Other films grown under intermediate precursor fluxes gave CL spectra similar to Figure 3c, although the peak associated with the band gap emission was of reduced intensity.

A higher resolution scan of the band gap region of the film in Figure 3c is shown in Figure 4. In addition to the CL measurement obtained at room temperature, a region scan was also performed on the sample after cooling with liquid nitrogen. At this reduced temperature the defect peak at ~368 nm was increased relative to the main band gap emission. The temperature dependence of this peak suggests that this is due to a thermally ionized shallow level defect caused by factors such as doping or point defects rather than a crystallographic defect.

The reasons for the differences in the CL spectra are not readily apparent from XRD and XPS. However TEM shows that there are small but significant differences in the structure of the films. Figure 5a is a TEM cross sectional image of the ZnS film with the strong band-gap emission, and it is evident from this image that the film is composed of large columns ~300−500 nm wide. Closer inspection of the film near the interface (Figure 5a inset) shows that the first ~ 200 nm of the

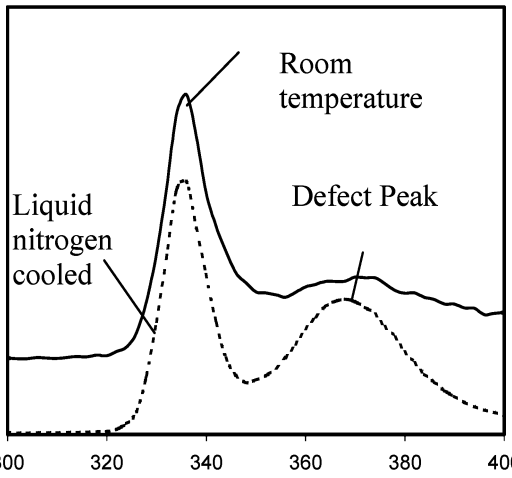

Figure 4. Region CL scan of a ZnS film with a strong band-gap emission. The CL scan is taken at both room temperature and at liquid nitrogen temperature.

film is composed of smaller columns roughly 100 nm wide. These small columns have a much higher density of shearing defects in the (111) plane than is present in the large columns. Figure 5b is a TEM cross sectional image of the thin film with no band-gap emission. It is readily apparent from this image that the structure of this film is dominated by the smaller columns with a higher density of shear defects. Since the film which produced the band-gap emission consisted of a combination of large, defect-free columns and smaller, more defective columns, and the non band-gap emission film only contained the latter; it is surmised that CL emission can be used to provide some insight into the properties of the columns. Additionally, threading defects (shown in Figure 5c) were observed throughout the non band-gap emission film as well as in the small column section of the band-gap emission film. These threading defects are evidence of an additional mismatch stress that is not present in the large columns in the band-gap emission film. Given that the Monte Carlo simulations found that the electron beam has a penetration depth of ~2.5 microns, it is fair to assume that the structure throughout the entire film influenced the CL spectra.

Studies correlating the defects with the cathodoluminescent response have identified a number of defect types for ZnS films grown on GaAs substrates.[14−15] It was found that shear defects produced only a very small (~4 nm) shift in the band gap whereas lattice mismatch defects (observed in single-source CVD films as threading defects) served as a non-radiative recombination center. This explains why there is no band gap emission observed in the film in Figure 3b; this film, although highly crystalline and oriented, contains threading defects. The film with the strong band gap emission since threading defects were only present in the small columns near the interface and not in the large columns that comprise the bulk of the film.

However, threading defects do not explain the broad peak at ~636 nm observed in all films. To determine the nature of this emission, monochromatic CL emission mapping was performed on the film with the strong band gap emission. Figure 6a is the planar SEM image of the surface of such a film. From this image it is evident that the film is grainy with elevated regions that most likely coincide with the tops of columns seen in the cross sectional TEM images in Figure 5a. Figure 6b is a monochromatic CL emission image of the same region of the film shown in Figure 6a, taken using the band gap emission wavelength of

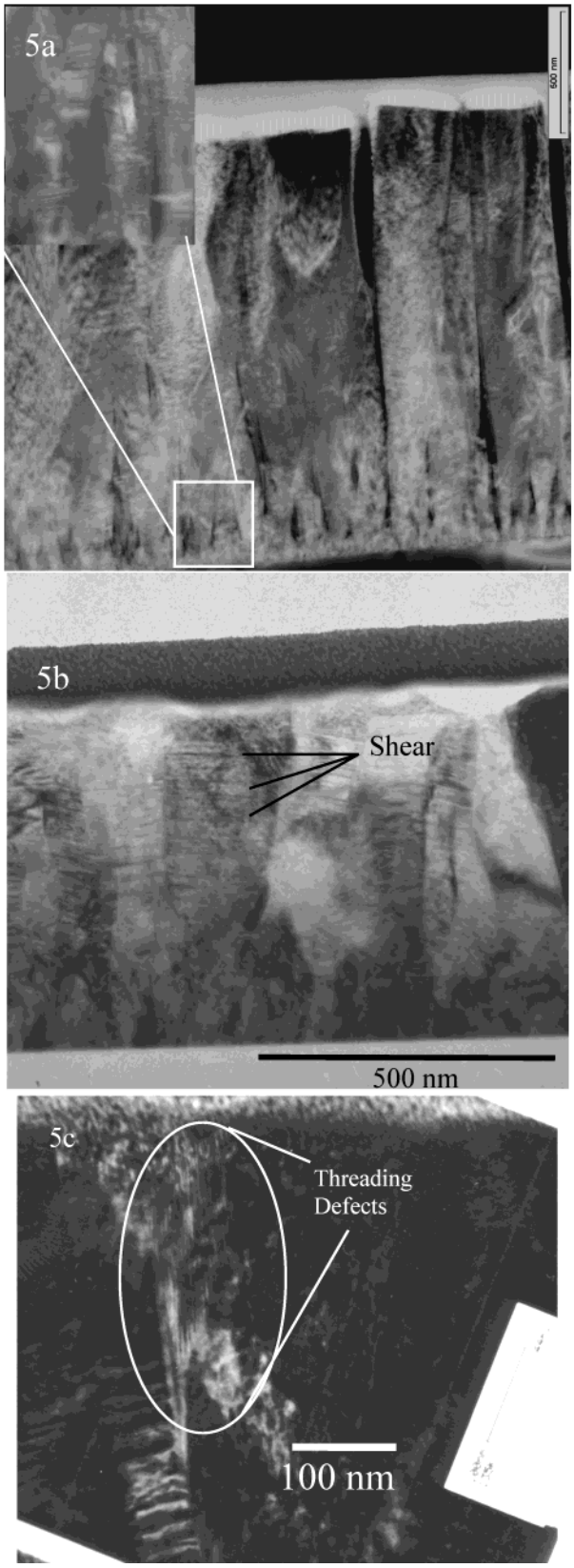

Figure 5. TEM cross-sectional images of: 5a) the ZnS film with a strong band-gap emission, 5b) the ZnS film with no band-gap emission, and 5c) bulk threading defects on the ZnS film with no band-gap emission.

336 nm. Figure 6c is a similar mono CL emission mapping image except that it measures light at 366 nm (the emission due to the side peak observed in figs. 3c and 4) and Figure 6d

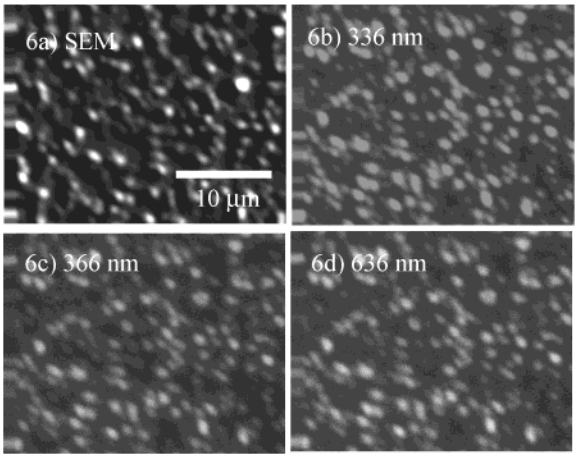

Figure 6. Surface SEM and CL images of the ZnS film with a strong band-gap emission: 6a) SEM images of surface of the film, 6b) CL emission image taken at 336 nm, 6c) CL emission image taken at 366 nm and 6d) CL emission image taken at 636 nm.

is the emission image observed at 636 nm. It is important to note that the images presented are done so with maximum contrast: the actual difference in intensity between light and dark areas in these images is minimal as all parts of the film emitted strongly. The interesting feature of these images is that figures 6b, 6c, and 6d are similar enough to be superimposable with the SEM image. This would suggest that, given the spatial resolution of the technique, the emission at ~636 nm is not due to individual defective columns.

The most likely cause for the ~636 nm emission observed in all films is the surface structure of the ZnS film. The XPS indicates high levels of carbon on the surface. Previous studies using in situ growth and analysis of single-source CVD films have shown that this carbon originates from the decomposition of the precursor.[16] Subsequent studies have also concluded, through correlating crystallite size and defect concentration, that carbon migration to the grain boundaries occurs during crystallite growth leaving the inside of the crystallites carbon-free.[17] It is highly likely that this high carbon surface region has a distorted or otherwise significantly different crystallographic structure to the bulk of the film, resulting in the broad and non band gap emission observed at ~636 nm.

IV. Conclusion

This study has shown that it is possible, under carefully controlled conditions, to grow cathodoluminescent ZnS films with strong band gap emissions in a one-step process with single-source CVD. Such a technique may provide a simple, safe, and low cost alternative of producing device grade ZnS films for light emitting applications.

Acknowledgment. The authors would like to thank Assoc. Prof. Matthew Phillips at the University of Technology Sydney for his help in analysis and advice.

References and Notes

(1) Nanda, J.; Sarma, D. D. *J. Appl. Phys.* **2001**, *90* (5), 2504.
(2) Khosravi, A.; Kundu, M.; Jatwa, L.; Deshpande, S. K.; Bhagwat, U. A.; Sastry, M.; Kulkarni, S. K. *Appl. Phys. Lett.* **1995**, *67* (18), 2702.
(3) Yamaga, S. *Physica B* **1993**, *185*, 500.
(4) Sohn, S. H.; Hamakawa, J. *J. Appl. Phys.* **1992**, *72* (6), 2492.
(5) Tran, N. H.; Lamb, R. N.; Mar, G. L. *Colloids Surf., A* **1999**, *155* (1), 93.
(6) Tran, N. H.; Hartmann, A. J.; Lamb, R. N. *J. Phys. Chem. B* **2002**, *106* (2), 352.
(7) Tran, N. H.; Hartmann, A. J.; Lamb, R. N. *J. Phys. Chem. B* **2000**, *104* (6), 1150.
(8) Gleizes, A. N. *Chem. Vap. Deposition* **2000**, *6* (4), 155.
(9) Pike, R. D.; Cui, H.; Kershaw, R.; Dwight, K.; Wold, A.; Blanton, T. N.; Wernberg, A. A.; Gysling, H. J. *Thin Solid Films* **1993**, *224*, 221.
(10) Nomura, R.; Murai, T.; Toyosaki, T.; Matsuda, H. *Thin Solid Films* **1995**, *271*, 4.
(11) Barreca, D.; Tondello, E.; Lydon, D.; Spalding, T. R.; Fabrizio, M. *Chem. Vapor Deposition* **2003**, *9* (2), 93.
(12) Lee, E. Y. M.; Tran, N. H.; Russell, J. J.; Lamb, R. N. *J. Phys. Chem. B* **2003**, *107* (22), 5208.
(13) Sze, S. M. *Physics of Semiconductor Device*; Wiley Interscience Publication: New York, 1981, 848.
(14) Mitsui, T.; Yamamoto, N.; Tadokoro, T.; Ohta, S. *J. Appl. Phys.* **1996**, *80* (12), 6972.
(15) Mitsui, T.; Yamamoto, N.; Yoshino, J.; Tadokoro, T.; Ohta, S.; Yanashima, K.; Inoue, K. *Appl. Surf. Sci.* **1996**, *100/101*, 625.
(16) Koch, M. H.; Hartmann, A. J.; Lamb, R. N.; Neuber, M.; Walz, J.; Grunze, M. *Surface Review and Lett.* **1997**, *4* (1), 39.
(17) Tran, N. H.; Hartmann, A. J.; Lamb, R. N. *J. Phys. Chem. B* **1999**, *103* (21), 4264.